

## OSR1-sensitive small intestinal Na<sup>+</sup> transport

Venkanna Pasham,\* Ganesh Pathare,\* Abul Fajol, Rexhep Rexhepaj, Diana Michael, Tatsiana Pakladok, Ioana Alesutan, Anand Rotte, Michael Föller, and Florian Lang

Department of Physiology, University of Tübingen, Tübingen, Germany

Submitted 8 September 2011; accepted in final form 21 September 2012

**Pasham V, Pathare G, Fajol A, Rexhepaj R, Michael D, Pakladok T, Alesutan I, Rotte A, Föller M, Lang F.** OSR1-sensitive small intestinal Na<sup>+</sup> transport. *Am J Physiol Gastrointest Liver Physiol* 303: G1212–G1219, 2012. First published September 27, 2012; doi:10.1152/ajpgi.00367.2011.—The oxidative stress responsive kinase 1 (OSR1) contributes to WNK (with no K)-dependent regulation of renal tubular salt transport, renal salt excretion, and blood pressure. Little is known, however, about a role of OSR1 in the regulation of intestinal salt transport. The present study thus explored whether OSR1 is expressed in intestinal tissue and whether small intestinal Na<sup>+</sup>/H<sup>+</sup> exchanger (NHE), small intestinal Na<sup>+</sup>-glucose cotransport (SGLT1), and/or colonic epithelium Na<sup>+</sup> channel (ENaC) differ between knockin mice carrying one allele of WNK-resistant OSR1 (*osr1*<sup>+/*KI*</sup>) and wild-type mice (*osr1*<sup>+/*+*</sup>). OSR1 protein abundance was determined by Western blotting, cytosolic pH from BCECF fluorescence, NHE activity from Na<sup>+</sup>-dependent realkalinization following an ammonium pulse, SGLT1 activity from glucose-induced current, and colonic ENaC activity from amiloride-sensitive transepithelial current in Ussing chamber experiments. As a result, OSR1 protein was expressed in small intestine of both *osr1*<sup>+/*KI*</sup> mice and *osr1*<sup>+/*+*</sup> mice. Daily fecal Na<sup>+</sup>, K<sup>+</sup>, and H<sub>2</sub>O excretion and jejunal SGLT1 activity were lower, whereas small intestinal NHE activity and colonic ENaC activity were higher in *osr1*<sup>+/*KI*</sup> mice than in *osr1*<sup>+/*+*</sup> mice. NHE3 inhibitor S-3226 significantly reduced NHE activity in both genotypes but did not abrogate the difference between the genotypes. Plasma osmolarity, serum antidiuretic hormone, plasma aldosterone, and plasma corticosterone concentrations were similar in both genotypes. Small intestinal NHE3 and colonic α-ENaC protein abundance were not significantly different between genotypes, but colonic phospho-β-ENaC (ser633) was significantly higher in *osr1*<sup>+/*KI*</sup> mice. In conclusion, OSR1 is expressed in intestine and partial WNK insensitivity of OSR1 increases intestinal NHE activity and colonic ENaC activity.

pH<sub>i</sub>; Na<sup>+</sup>/H<sup>+</sup> exchanger; ENaC; amiloride; WNT

THE OXIDATIVE STRESS RESPONSIVE KINASE 1 (OSR1) contributes to signaling of transport regulation during oxidative and osmotic stress (9, 25, 27, 40, 43, 47, 55). The kinase is phosphorylated and thus activated by the WNK (with no K) kinase isoforms WNK1 and WNK4, which are in turn activated by osmotic cell shrinkage (33, 40, 52, 59, 59), insulin (46), and antidiuretic hormone (ADH) (35). During evolution OSR1 was duplicated by the STE20/SPS1-related proline-alanine-rich kinase (SPAK) (7). Similar to SPAK (30), OSR1 upregulates the thiazide-sensitive Na<sup>+</sup>-Cl<sup>-</sup> cotransporter NCC (10) and the furosemide-sensitive Na<sup>+</sup>-K<sup>+</sup>-2Cl<sup>-</sup> cotransporter NKCC (2, 36), with both carriers contributing to increasing cell volume (29). By the same token, the kinases downregulate KCl cotransporters (15,

18, 27), i.e., carriers decreasing cell volume (23, 29). Moreover, OSR1 and SPAK increase the HCO<sub>3</sub><sup>-</sup> permeability of the cystic fibrosis transmembrane conductance regulator CFTR (34). GCK-3, a *Caenorhabditis elegans* ortholog of mammalian SPAK and OSR1 (6), inhibits the ClC anion channel CLH-3b (11). Owing to their influence on the respective transport systems, the kinases participate in the regulation of cell volume, transepithelial transport, renal salt excretion, migration, and GABA neurotransmission (3, 7, 9, 16, 20, 22, 26, 27, 40, 53).

Certain mutations of WNK1 and WNK4 result in hypertension (13, 14, 27, 49, 56) and autonomic neuropathy (27). OSR1 is similarly implicated in the regulation of blood pressure (17, 50–52) and is a potential drug target in the treatment of hypertension (12, 17, 40, 50).

OSR1 and SPAK upregulate the Na<sup>+</sup>-Cl<sup>-</sup> cotransporter and the Na<sup>+</sup>-K<sup>+</sup>-2Cl<sup>-</sup> cotransporter by phosphorylation of the carriers (9, 10, 26, 27, 30, 31, 35, 40, 49). The kinases phosphorylate the amino acid sequence [S/G/V]RFx[V/I]xx[V/I/T/S]xx, where x represents any amino acid (8). The carriers are phosphorylated at the conserved Ser/Thr residues in the NH<sub>2</sub>-terminal domain of the carrier proteins (31, 32, 35).

In *C. elegans*, OSR1 is expressed in intestine (47). Surprisingly though, to the best of our knowledge, nothing is known on the potential role of OSR1 in intestinal transport regulation. Intestinal Na<sup>+</sup> reabsorption is in large part accomplished by the small intestinal Na<sup>+</sup>/H<sup>+</sup> exchanger NHE3 (21, 58), colonic Na<sup>+</sup> reabsorption involves the amiloride-sensitive epithelial Na<sup>+</sup> channel ENaC (28). Notably, in *wnk4*<sup>D561A/+</sup> knockin mice the increased phosphorylation of the kinases OSR1 and SPAK and increased apical expression of phosphorylated Na<sup>+</sup>-Cl<sup>-</sup> cotransporter in the renal distal convoluted tubules was paralleled by an increased activity of ENaC in the kidney (57).

The present study thus explored the role of OSR1 in the regulation of small intestinal Na<sup>+</sup>/H<sup>+</sup> exchanger (NHE) activity as well as amiloride-sensitive Na<sup>+</sup> current in the terminal colon. To this end, experiments were performed in heterozygous OSR1 knockin mice resistant to WNK-mediated activation (*osr1*<sup>+/*KI*</sup>) and wild-type mice (*osr1*<sup>+/*+*</sup>) (38). The *osr1*<sup>+/*KI*</sup> mice may have decreased OSR1 activity; however, OSR1 protein expression is unaltered (48). As indicated earlier (38), homozygous OSR1 knockin mice (*osr1*<sup>KI/KI</sup>) are not viable.

### MATERIALS AND METHODS

**Animals.** All animal experiments were conducted according to the German law for the welfare of animals and were approved by local authorities. Blood was drawn or tissue isolated from sex-matched 2- to 9-mo-old heterozygous OSR1 knockin mice (*osr1*<sup>+/*KI*</sup>) and wild-type mice (*osr1*<sup>+/*+*</sup>), kindly provided by Dario Alessi from the MRC Protein Phosphorylation Unit, College of Life Sciences, University of Dundee, Dundee, UK. As described earlier (38), in the knockin mice the T-loop Thr residue in OSR1 (Thr185) was mutated to Ala to

\* V. Pasham and G. Pathare contributed equally and thus share first authorship.

Address for reprint requests and other correspondence: F. Lang, Dept. of Physiology, Univ. of Tübingen, Gmelinstr. 5, D-72076 Tübingen, Germany (e-mail: florian.lang@uni-tuebingen.de).

Table 1. Serum ADH, plasma aldosterone, and plasma corticosterone concentrations in *osr1*<sup>+/-KI</sup> and *osr1*<sup>+/-+</sup> mice

	<i>osr1</i> <sup>+/-+</sup>	<i>osr1</i> <sup>+/-KI</sup>
ADH, ng/ml	0.99 ± 0.14	1.04 ± 0.16
Aldosterone, pg/ml	172.6 ± 15.1	198.3 ± 13.4
Corticosterone, pg/ml	352.6 ± 69.8	369.6 ± 43.4

Values are arithmetic means ± SE (*n* = 6). ADH, antidiuretic hormone; *osr1*<sup>+/-KI</sup>, OSR1 knockin mice; *osr1*<sup>+/-+</sup>, wild-type mice.

prevent activation by WNK isoforms. Mice had free access to control diet (Walkermühle, Hechingen, Germany) and tap drinking water ad libitum. To obtain blood, mice were anesthetized with diethylether (Roth, Karlsruhe, Germany) and blood specimens were drawn from the retroorbital plexus into capillaries. To obtain tissue, the animals were anesthetized with diethylether and euthanized by cervical dislocation. Prior to further use, small intestinal segments were washed to remove fecal material.

**Antibodies.** Anti-OSR1 (1:900) (48), kindly provided by D. Alessi (University of Dundee); polyclonal anti-epithelial  $\alpha$ -ENaC (1:500) (Abcam); polyclonal antibody against sodium channel protein (pan) 1:800 (Acris Antibodies), anti-phospho- $\beta$  ENaC (SCNN1B; Ser633) polyclonal (1:400) (Bioss Antibodies), NHE3 (1:1,000) (Nobis Biologicals),  $\beta$ -actin (1:1,000) (Cell Signaling Technology, Frankfurt, Germany), GAPDH (1:3,000) (Cell Signaling Technology), horseradish peroxidase (HRP)-linked anti-rabbit (1:2,000) (Cell Signaling Technology), and anti-mouse secondary antibody (1:2,000) (GE Healthcare, Freiburg, Germany) were used.

**Determination of serum ADH, aldosterone, and corticosterone concentrations.** Serum ADH concentration was determined by utilizing a commercial EIA kit (AVP EIA Kit, Phoenix Europe, Karlsruhe, Germany). The plasma aldosterone and corticosterone concentrations were determined by using a commercial radioimmunoassay kit (Demeditec, Kiel, Germany). All kits were used according to the manufacturer's instructions.

**Western blotting.** Mice were euthanized by cervical dislocation under ether anesthesia, and the abdomen was opened. The small intestine was cut longitudinally. The tissue was homogenized with an electric homogenizer at 4°C in lysis buffer [54.6 mM HEPES; 2.69 mM Na<sub>4</sub>P<sub>2</sub>O<sub>7</sub>; 360 mM NaCl; 10% (vol/vol) glycerol; 1% (vol/vol) Nonidet P-40] containing phosphatase and protease inhibitors (Roche, Mannheim, Germany). The small intestinal brush border membrane was prepared as described before (44).

Homogenates were clarified by centrifugation at 14,000 rpm for 20 min. The samples containing 100  $\mu$ g protein were subjected to 10% SDS-PAGE and blotted onto nitrocellulose membranes (Schleicher & Schuell). The membranes were blocked for 2 h in Tris-buffered saline (TBS) containing 7% fat-free powder milk. Then, the membranes were incubated overnight with primary antibody against mouse OSR1 (residues 389–408 SAHLQPAGQMPTQPAQVSL, S149C, detecting a molecule of ~58 kDa; Ref. 48) and GAPDH followed by incubation with secondary HRP anti-mouse IgG. All antibodies were diluted in TBS containing 5% milk.

**Small intestinal NHE3 activity.** For the isolation of ileal villi, animals were fasted for 6 h prior to the experiments. After euthanasia the terminal 2 cm of the ileum were removed and cut longitudinally. After wash with standard HEPES solution the small intestine was sliced into 0.3-cm<sup>2</sup> sections. The tissues were transferred onto the cooled stage of a dissecting microscope and the individual villi were detached from the small intestine by snapping off the ileal base with sharpened microdissection tweezers. Care was taken not to touch the apical part of the villi. The villi were attached to a glass coverslip precoated with Cell-Tak adhesive (BD Biosciences, Heidelberg, Germany). For quantitative digital imaging of cytosolic pH (pH<sub>i</sub>), isolated individual villi were incubated in a HEPES-buffered Ringer solution containing 10  $\mu$ M 2',7'-bis-(carboxyethyl)-5(6)-carboxyfluorescein-

acetoxymethylester (BCECF-AM; Molecular Probes, Leiden, The Netherlands) for 15 min at 37°C. After loading, the chamber was flushed for 5 min with Ringer solution to remove any deesterified dye sticking to the outside of the villi (42). The perfusion chamber was mounted on the stage of an inverted microscope (Axiovert 135, Zeiss, Göttingen, Germany), which was used in the epifluorescence mode with a  $\times 40$  oil immersion objective (Neoplan, Zeiss). BCECF was successively excited at 490/10 and 440/10 nm, and the resultant fluorescent signal was monitored at 535/10 nm by use of an intensified charge-coupled device camera (Proxitronic, Bensheim, Germany) and specialized computer software (Metafluor, Puchheim, Germany). Individual cells from the brush border of the villi were outlined and monitored during the course of the measurement. Intensity ratio data (490/440) were converted into pH values by the high-K<sup>+</sup>/nigericin calibration technique (54). To this end, the cells were perfused at the end of each experiment for 5 min with standard high-K<sup>+</sup>/nigericin (10  $\mu$ g/ml) solution (pH 7.0). The intensity ratio data thus obtained were converted into pH values by using the *r*<sub>max</sub>, *r*<sub>min</sub>, and p*K*<sub>a</sub> values previously generated from calibration experiments to generate a standard nonlinear curve (pH range 5 to 8.5).

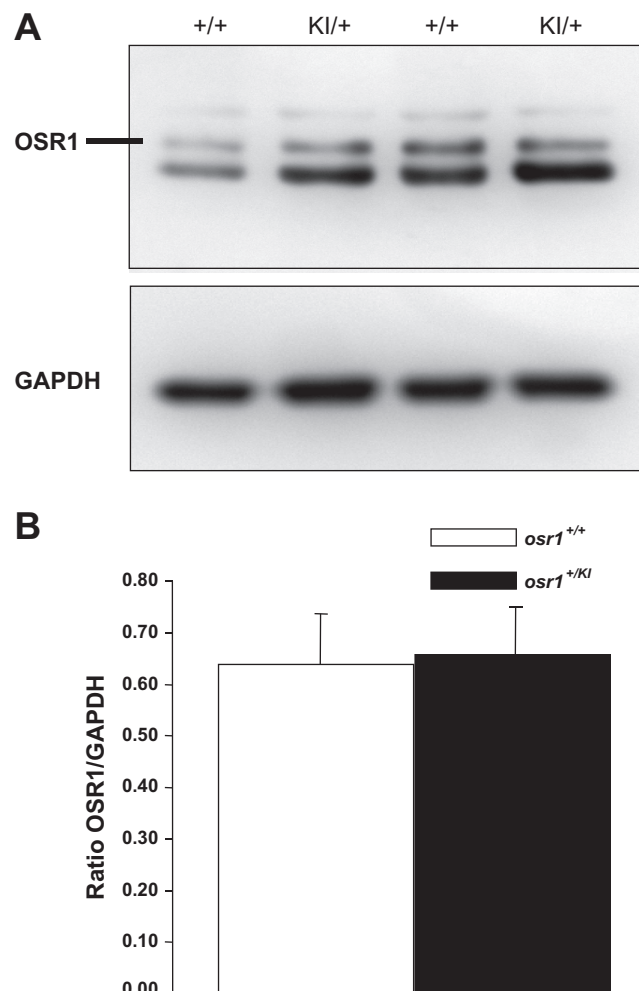


Fig. 1. Expression of oxidative stress response kinase 1 (OSR1) in small intestinal tissue from wild-type (*osr1*<sup>+/-+</sup>) mice and knockin mice carrying one allele of WNK-resistant OSR1 (*osr1*<sup>+/-KI</sup>). A: original Western blot (*n* = 4 for each genotype) of the expression of OSR1 protein (top) and GAPDH protein (bottom) in the small intestine from heterozygous OSR1 knockin mice (+/-KI) and wild-type mice (+/+). B: arithmetic means ± SE (*n* = 4 for each genotype) of abundance of OSR1 (relative to GAPDH) in small intestinal tissue from *osr1*<sup>+/-+</sup> (open bar) and *osr1*<sup>+/-KI</sup> (solid bar) mice.

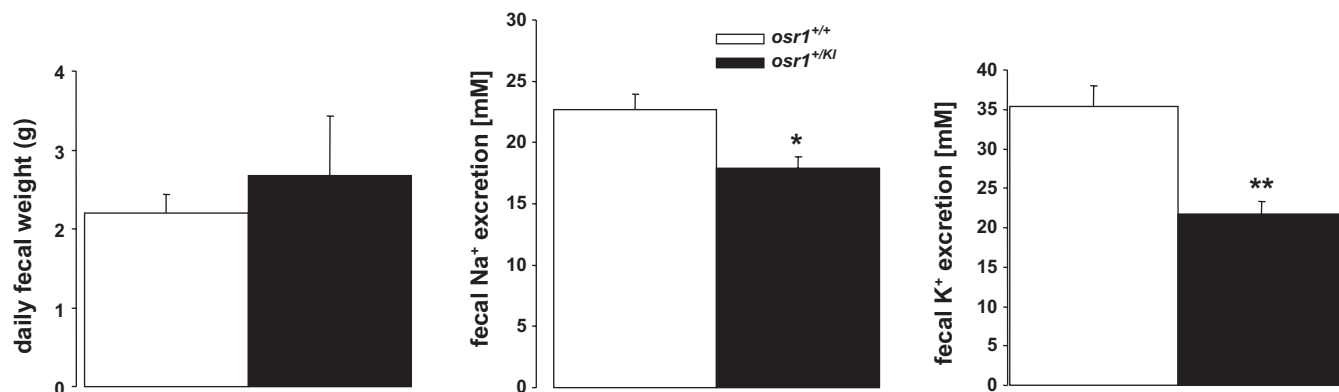


Fig. 2. Fecal weight and  $\text{Na}^+$  and  $\text{K}^+$  excretion in *osr1*<sup>+/+</sup> and *osr1*<sup>+/KI</sup> mice. Arithmetic means  $\pm$  SE ( $n = 10$ – $11$ ) of daily fecal weight (left), fecal  $\text{Na}^+$  excretion (middle) and fecal  $\text{K}^+$  excretion (right) in heterozygous OSR1 knockin mice (solid bars) and wild-type mice (open bars). \*Significant difference from *osr1*<sup>+/+</sup> mice (Student's *t*-test,  $P < 0.05$ ).

For acid loading, cells were transiently exposed to a solution containing 20 mM  $\text{NH}_4\text{Cl}$  leading to initial alkalization of  $\text{pH}_i$  due to entry of  $\text{NH}_3$  and binding of  $\text{H}^+$  to form  $\text{NH}_4^+$  (41). The acidification of cytosolic  $\text{pH}$  upon removal of ammonia allowed calculating the mean intrinsic buffering power ( $\beta$ ) of the cells (41). Assuming that  $\text{NH}_4^+$  and  $\text{NH}_3$  are in equilibrium in cytosolic and extracellular fluid and that ammonia leaves the cells as  $\text{NH}_3$ :

$$\beta = \Delta[\text{NH}_4^+]_i / \Delta\text{pH}_i,$$

where  $\Delta\text{pH}_i$  is the decrease of  $\text{pH}_i$  following ammonia removal and  $\Delta[\text{NH}_4^+]_i$  is the decrease of cytosolic  $\text{NH}_4^+$  concentration, which is identical to the concentration of  $[\text{NH}_4^+]_i$  immediately before the removal of ammonia. The  $\text{pK}$  for  $\text{NH}_4^+/\text{NH}_3$  is 8.9 (5) and at an extracellular  $\text{pH}$  ( $\text{pH}_o$ ) of 7.4 the  $\text{NH}_4^+$  concentration in extracellular fluid ( $[\text{NH}_4^+]_o$ ) is 19.37 mM [ $20/(1 + 10^{\text{pH}_o - \text{pK}})$ ]. The intracellular  $\text{NH}_4^+$  concentration ( $[\text{NH}_4^+]_i$ ) was calculated from

$$[\text{NH}_4^+]_i = 19.37 \cdot 10^{\text{pH}_o - \text{pH}_i} \text{ mM}$$

To calculate the  $\Delta\text{pH}/\text{min}$  during realkalinization, a manual linear fit was placed over a narrow  $\text{pH}$  range ( $\text{pH}$  6.7 to 6.9), which could be applied to all measured cells.

The solutions were composed (in mM) as follows: standard HEPES: 115 NaCl, 5 KCl, 1  $\text{CaCl}_2$ , 1.2  $\text{MgSO}_4$ , 2  $\text{NaH}_2\text{PO}_4$ , 10 glucose, 32.2 HEPES; sodium-free HEPES: 132.8 *N*-methyl-D-glucamine (NMDG), 3 KCl, 1  $\text{CaCl}_2$ , 1.2  $\text{MgSO}_4$ , 2  $\text{KH}_2\text{PO}_4$ , 32.2 HEPES, 10 mannitol, 10 glucose (for sodium-free ammonium chlo-

ride, 10 mM NMDG and mannitol were replaced with 20 mM  $\text{NH}_4\text{Cl}$ ); high  $\text{K}^+$  for calibration 105 KCl, 1  $\text{CaCl}_2$ , 1.2  $\text{MgSO}_4$ , 32.2 HEPES, 10 mannitol, 5  $\mu\text{M}$  nigericin. The  $\text{pH}$  of the solutions was titrated to 7.4 or 7.0 with HCl/NaOH, HCl/NMDG, and HCl/KOH, respectively, at 37°C. The NHE3 inhibitor s3226 was a kind gift of Hoechst (Frankfurt, Germany).

**Ussing chamber experiments.** ENaC activity was estimated from the amiloride-sensitive potential difference across the colonic epithelium. After removal of the outer serosal and the muscular layer of distal colon under a microscope, tissues were mounted onto a custom-made mini-Ussing chamber with an opening diameter of 0.99 mm and an opening area of 0.00769  $\text{cm}^2$ . The serosal and luminal perfusate contained (in mM) 145 NaCl, 1  $\text{MgCl}_2$ , 2.6 Ca-gluconate, 0.4  $\text{KH}_2\text{PO}_4$ , 1.6  $\text{K}_2\text{HPO}_4$ , 5 glucose. To assess ENaC-mediated transport, 50  $\mu\text{M}$  amiloride (in ethanol; Sigma, Schnellendorf, Germany) was added to the luminal perfusate. Before mounting the tissue into the Ussing chamber, the empty chamber was placed into the apparatus, and the potential difference across the empty chamber was set to 0 mV. In all Ussing chamber experiments, the transepithelial potential difference ( $V_t$ ) was determined continuously, and the apparent transepithelial resistance ( $R_t$ ) was estimated from the voltage deflections ( $\Delta V_t$ ) elicited by imposing test currents ( $I_t$ ) of 1  $\mu\text{A}$ . The resulting  $R_t$  was calculated according to Ohm's law. For the determination of the  $R_t$  the resistance of the empty chamber was subtracted.

**Fecal weight,  $\text{Na}^+$ , and  $\text{K}^+$ .** Fecal  $\text{Na}^+$  was analyzed as described previously (39). Briefly, feces was collected in metabolic cages

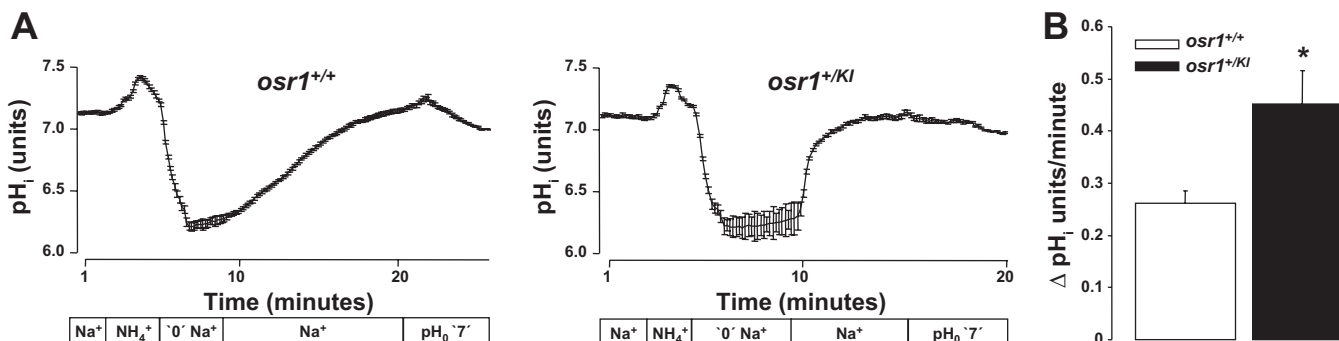


Fig. 3. pH recovery following an ammonium pulse in ileum from *osr1*<sup>+/+</sup> and *osr1*<sup>+/KI</sup> mice. Alterations of cytosolic  $\text{pH}$  ( $\Delta\text{pH}$ ) in ileal epithelial cells following an ammonium pulse. To load the cells with  $\text{H}^+$ , 20 mM  $\text{NH}_4\text{Cl}$  was added and  $\text{Na}^+$  removed [replaced by *N*-methyl-D-glucamine (NMDG)] in a first step,  $\text{NH}_4\text{Cl}$  removed in a second step,  $\text{Na}^+$  added in a third step, and nigericin applied in a fourth step to calibrate each individual experiment. A: representative experiments showing time-dependent alterations of  $\text{pH}$  in isolated small intestinal villi from heterozygous OSR1 knockin mice (right) and wild-type mice (left). B: arithmetic means  $\pm$  SE ( $n = 8$ ) of sodium-dependent  $\text{pH}$  recovery in enterocytes from small intestine of *osr1*<sup>+/+</sup> (open bars) and *osr1*<sup>+/KI</sup> (solid bars) mice. \*Significant difference from *osr1*<sup>+/+</sup> mice (Student's *t*-test,  $P < 0.05$ ).



Table 2.  $\text{pH}_i$ , buffer capacity, and  $\text{Na}^+$ -independent pH recovery in intestinal epithelial cells from  $\text{osr1}^{+/KI}$  and  $\text{osr1}^{+/+}$  mice

	$\text{pH}_i$	Buffer Capacity, mM/pH unit	$\text{Na}^+$ Independent pH Recovery, $\Delta \text{pH}$ units/min	Number of Mice	Number of Cells
$\text{osr1}^{+/+}$	$7.11 \pm 0.03$	$27.9 \pm 5.2$	$0.008 \pm 0.012$	8	120
$\text{osr1}^{+/KI}$	$7.10 \pm 0.02$	$24.4 \pm 3.0$	$0.012 \pm 0.018$	8	133

Values are means  $\pm$  SE.  $\text{pH}_i$ , cytosolic pH.

(Techniplast, Hohenpeissenberg, Germany). Fecal dry weight was taken after drying the sample at  $80^\circ\text{C}$  for  $\sim 3$  h. Then the dried feces was dissolved in 5 ml of 0.75 M nitric acid and shaken for 48 h to yield a homogenous creamy mass. The sample was then centrifuged at  $\sim 2,500$  g for 10 min, and 1 ml of the supernatant was again centrifuged at  $\sim 10,000$  rpm for 5 min. Aliquots from the second supernatant were stored at  $-20^\circ\text{C}$  until analysis. To obtain the absolute electrolyte content of the feces in micromole, the measured electrolyte concentration (using a AFM 5051 flame photometer, Eppendorf, Germany) was multiplied by 5.

**Electrogenic glucose transport.** For the analysis of electrogenic small intestinal glucose transport, jejunal segments were mounted into a custom-made mini-Ussing chamber with an opening of  $0.00769$   $\text{cm}^2$ . Under control conditions, the serosal and luminal perfusate contained (in mM) 115 NaCl, 2 KCl, 1  $\text{MgCl}_2$ , 1.25  $\text{CaCl}_2$ , 0.4  $\text{KH}_2\text{PO}_4$ , 1.6  $\text{K}_2\text{HPO}_4$ , 5 Na pyruvate, 25  $\text{NaHCO}_3$ , 20 mannitol (pH 7.4, NaOH). To induce current, glucose (20 mM) was added to the luminal perfusate at the expense of mannitol. Before mounting the tissue into the Ussing chamber, we placed the empty chamber into the apparatus and the potential difference across the empty chamber

set to 0 mV. In all Ussing chamber experiments the  $V_t$  was determined continuously and apparent  $R_t$  was estimated from the  $\Delta V_t$  elicited by imposing  $I_t$ . The resulting  $R_t$  was calculated according to Ohm's law. For the determination of the  $R_t$  in the presence of mannitol or glucose, the resistance of the empty chamber was subtracted. The glucose-induced current was calculated as the difference between the current in the presence of 20 mM glucose and 20 mM mannitol.

**Immunohistochemistry.** The colons from  $\text{osr1}^{+/+}$  and  $\text{osr1}^{+/KI}$  mice were perfused with 4% PFA/PBS, cryoprotected in 30% sucrose at  $4^\circ\text{C}$  overnight, and frozen in Tissue-Tek (Sakura Finetek). For immunohistochemistry, colon sections of 8  $\mu\text{m}$  were dried at room temperature for 30 min and fixed for 15 min RT in 4% paraformaldehyde/PBS. Slides were rinsed three times in PBS, permeabilized with 0.5% Triton X-100/PBS for 10 min at room temperature, pre-blocked with 10% normal goat serum in PBS for 1 h at room temperature, and incubated overnight at  $4^\circ\text{C}$  with the primary rabbit polyclonal anti- $\alpha$ -ENaC antibody (1:500, Abcam). The primary antibody was detected with fluorescence-labeled secondary goat anti-rabbit-FITC conjugated antibody (1:1,000, Invitrogen) for 1 h at room temperature. Nuclei were stained with DRAQ-5 dye (1:2,000, Biosta-

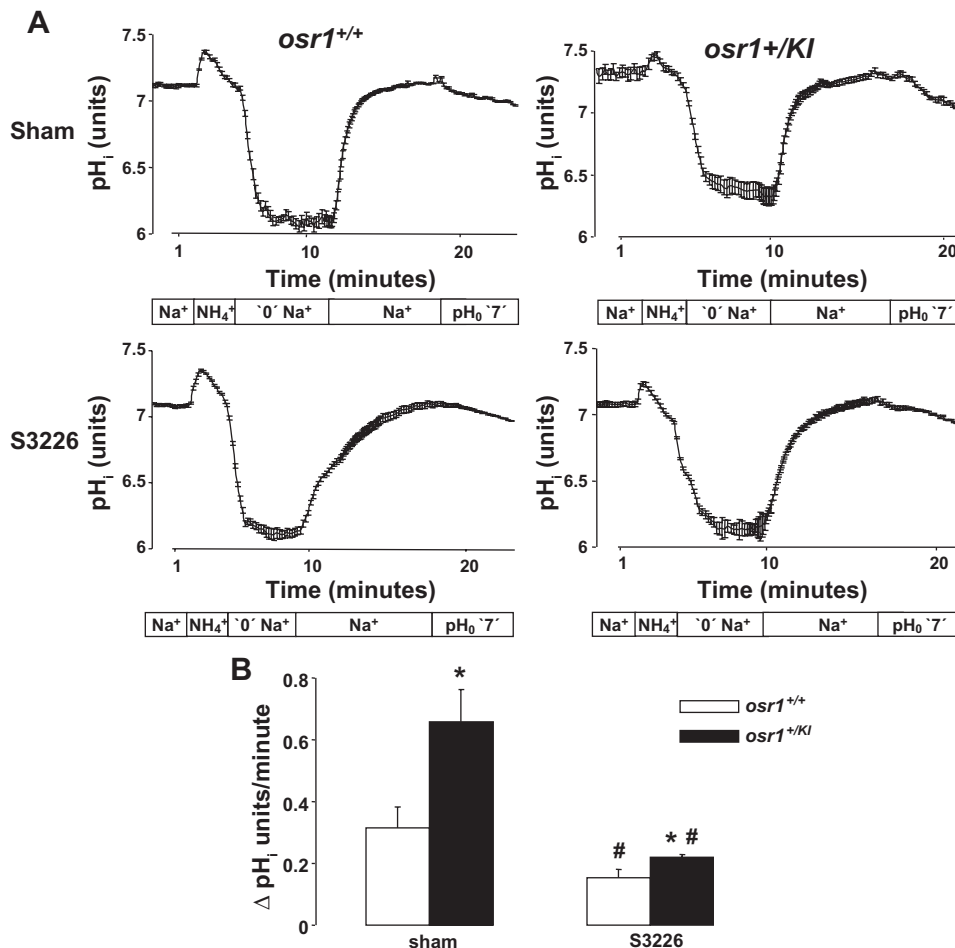


Fig. 4. Effect of S3226 on the pH recovery following an ammonium pulse in ileum from  $\text{osr1}^{+/+}$  and  $\text{osr1}^{+/KI}$  mice. A: representative experiments showing time-dependent alterations of pH in isolated small intestinal villi from heterozygous OSR1 knockin mice (right) and wild-type mice (left) in the absence (sham, top) and presence (bottom) of S3226. B: arithmetic means  $\pm$  SE ( $n = 9$ ) of sodium-dependent pH recovery in enterocytes from small intestine of  $\text{osr1}^{+/+}$  (open bars) and  $\text{osr1}^{+/KI}$  (solid bars) mice. \*Significant difference from  $\text{osr1}^{+/+}$  mice (Student's  $t$ -test,  $P < 0.05$ ); #significant difference from respective sham treatment.

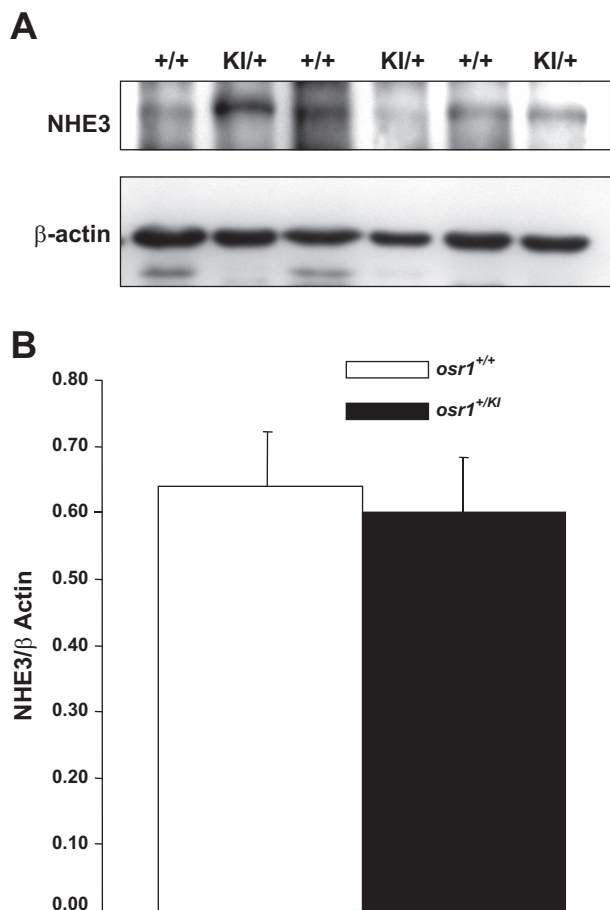


Fig. 5. Expression of NHE3 in small intestinal brush border membrane preparations from *osr1*<sup>+/+</sup> and *osr1*<sup>KI/+</sup> mice. A: original Western blot ( $n = 3$  for each genotype) of the expression of NHE3 protein (top) and  $\beta$ -actin protein (bottom) in the small intestine from heterozygous OSR1 knockin mice and wild-type mice. B: arithmetic means  $\pm$  SE ( $n = 3$  for each genotype) of abundance of NHE3 (relative to  $\beta$ -actin) in small intestinal tissue from *osr1*<sup>+/+</sup> (open bar) and *osr1*<sup>KI/+</sup> (solid bar) mice.

tus, Leicestershire, UK). The slides were mounted with ProLong Gold antifade reagent (Invitrogen). Images were taken on a Zeiss LSM5 EXCITER Confocal Laser Scanning Microscope (Carl Zeiss Micro-Imaging) with water immersion Plan-Neofluar $\times 40/1.3$  NA DIC.

**Statistics.** Data are provided as means  $\pm$  SE;  $n$  represents the number of independent experiments. All data were tested for significance by Student's unpaired two-tailed  $t$ -test. Only results with  $P < 0.05$  were considered statistically significant.

## RESULTS

To uncover a role of the OSR1 in the regulation of small intestinal  $\text{Na}^+$  transport, experiments were performed in OSR1 knockin mice (*osr1*<sup>KI/+</sup>) that were heterozygously carrying a WNK-insensitive <sup>Thr185Ala</sup>OSR1 mutant. The animals were compared with wild-type mice (*osr1*<sup>+/+</sup>). Because OSR1 participates in renal salt transport regulation, plasma osmolarity as well as serum ADH, plasma aldosterone, and plasma corticosterone concentration were determined in *osr1*<sup>+/+</sup> and *osr1*<sup>KI/+</sup> mice to possibly reveal deranged regulation of electrolyte homeostasis. As listed in Table 1, no significant differences between the two genotypes were observed in serum ADH, plasma aldosterone, and plasma corticosterone concentrations.

A next series of experiments explored the expression of OSR1 in the small intestine from *osr1*<sup>+/+</sup> and *osr1*<sup>KI/+</sup> mice. As shown in Fig. 1, OSR1 protein was expressed in both *osr1*<sup>KI/+</sup> mice and *osr1*<sup>+/+</sup> mice. The band reflecting OSR1 protein is 58 kDa. The additional bands may reflect unspecific staining. OSR1 is expressed in small intestinal tissue of both *osr1*<sup>+/+</sup> and *osr1*<sup>KI/+</sup> mice. The band density was similar in *osr1*<sup>+/+</sup> and *osr1*<sup>KI/+</sup> mice; the Western blot does not, however, rule out minor differences between *osr1*<sup>+/+</sup> and *osr1*<sup>KI/+</sup> mice. A recent study demonstrated unaltered expression of OSR1 even in homozygous *osr1*<sup>KI/KI</sup> embryonic stem cells (48).

In a first approach to estimate intestinal  $\text{Na}^+$  transport, the daily fecal  $\text{Na}^+$  excretion was determined. As a result, the fecal  $\text{Na}^+$  output was significantly lower in *osr1*<sup>KI/+</sup> mice than in *osr1*<sup>+/+</sup> mice (Fig. 2). The daily fecal  $\text{K}^+$  excretion was similarly lower in *osr1*<sup>KI/+</sup> mice than in *osr1*<sup>+/+</sup> mice (Fig. 2). The weight of the feces was similar in *osr1*<sup>+/+</sup> mice and in *osr1*<sup>KI/+</sup> mice (Fig. 2). The decreased fecal  $\text{Na}^+$  and  $\text{K}^+$  excretion in *osr1*<sup>KI/+</sup> mice was paralleled by a decrease of fecal water excretion. The fecal water content was significantly lower in *osr1*<sup>KI/+</sup> mice ( $43.1 \pm 4.8\%$ ,  $n = 7$ ) than in wild-type mice ( $56.2 \pm 2.2\%$ ,  $n = 6$ ).

To test whether increased small intestinal absorption of  $\text{Na}^+$  in *osr1*<sup>KI/+</sup> mice was due to increased activity of sodium glucose cotransporter (SGLT1), glucose-induced current in jejunal tissue was measured by use of an Ussing chamber. As a result, the glucose-induced current was significantly ( $P < 0.01$ ) lower in *osr1*<sup>KI/+</sup> mice ( $-1,622 \pm 143 \mu\text{A}/\text{cm}^2$ ,  $n = 10$ ) than in *osr1*<sup>+/+</sup> mice ( $-2,226 \pm 141 \mu\text{A}/\text{cm}^2$ ,  $n = 8$ ).

The major small intestinal mechanisms accomplishing small intestinal  $\text{Na}^+$  reabsorption is the NHE. To estimate NHE activity, the pH recovery following an ammonium pulse was determined in ileum from *osr1*<sup>+/+</sup> and *osr1*<sup>KI/+</sup> mice. Figure 3 illustrates the alterations of  $\text{pH}_i$  during this maneuver. Prior to the maneuver,  $\text{pH}_i$  was similar in *osr1*<sup>+/+</sup> mice and *osr1*<sup>KI/+</sup> mice (Table 2). In both genotypes the application of 20 mM

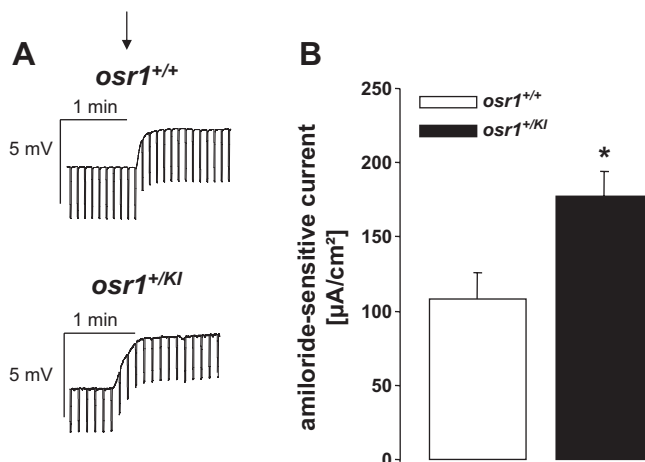


Fig. 6. Amiloride-sensitive transepithelial current in distal colon from *osr1*<sup>+/+</sup> and *osr1*<sup>KI/+</sup> mice. A: representative original tracings of the transepithelial colonic potential difference in heterozygous OSR1 knockin mice and wild-type mice. An arrow highlights the addition of amiloride. B: arithmetic means  $\pm$  SE ( $n = 10$ –12) of the amiloride-sensitive equivalent short-circuit current in distal colonic epithelium from *osr1*<sup>+/+</sup> (open bar) and *osr1*<sup>KI/+</sup> (solid bar) mice. \*Significant difference from *osr1*<sup>+/+</sup> mice (Student's  $t$ -test,  $P < 0.05$ ).

$\text{NH}_4\text{Cl}$  was followed by cytosolic alkalinization owing to entry of  $\text{NH}_3$  with subsequent binding of intracellular  $\text{H}^+$ . The following  $\text{NH}_4^+$  removal resulted in a sharp cytosolic acidification due to exit of  $\text{NH}_3$  with cellular retention of  $\text{H}^+$ . The buffer capacity was similar in *osr1*<sup>+/KI</sup> mice and *osr1*<sup>+/+</sup> mice. The cytosolic pH recovery in the absence of extracellular  $\text{Na}^+$  was negligible, indicating that small intestinal cells did not express functionally relevant  $\text{Na}^+$ -independent  $\text{H}^+$  extrusion mechanisms. The addition of  $\text{Na}^+$  was, however, followed by rapid realkalinization, pointing to the activity of the  $\text{Na}^+/\text{H}^+$  exchanger NHE3. The alkalinization was significantly more rapid in *osr1*<sup>+/KI</sup> mice than in *osr1*<sup>+/+</sup> mice (Fig. 3, A and B), pointing to enhanced NHE activity in *osr1*<sup>+/KI</sup> mice.

To test for the contribution of NHE3 to the observed NHE activity, a further series of experiments was performed using the specific NHE3 inhibitor s3226 at a concentration of 10  $\mu\text{M}$ . In the absence of s3226 the sodium-dependent pH recovery was significantly higher in *osr1*<sup>KI/+</sup> mice than in *osr1*<sup>+/+</sup> mice (Fig. 4). The addition of s3226 significantly reduced the sodium-dependent pH recovery in both *osr1*<sup>+/+</sup> mice and *osr1*<sup>KI/+</sup> mice (all values:  $n = 9$ ) but did not abolish the difference between

the genotypes. Accordingly, the sodium-dependent pH recovery was still significantly higher in *osr1*<sup>+/KI</sup> mice after S3226 treatment (Fig. 4B). Furthermore, Western blot analysis of small intestinal brush border membrane revealed that membrane abundance of NHE3 was not different between the genotypes ( $n = 12$ , Fig. 5).

The fecal  $\text{Na}^+$  excretion is also modified by colonic  $\text{Na}^+$  reabsorption via the amiloride-sensitive apical  $\text{Na}^+$  channel ENaC. Amiloride was used at 50  $\mu\text{M}$ , a concentration fully inhibiting ENaC but too low to inhibit NHE3 activity ( $\text{IC}_{50} > 100 \mu\text{M}$ ; Ref. 45). The amiloride-sensitive  $\text{Na}^+$  transport through this channel generates a lumen-negative transepithelial potential and a transepithelial current. As shown in Fig. 6, the amiloride-sensitive equivalent short-circuit current in distal colonic epithelium was significantly higher in colonic tissue from *osr1*<sup>+/KI</sup> mice than in colonic tissue from *osr1*<sup>+/+</sup> mice.

Additional experiments addressed the expression, localization, and phosphorylation of ENaC protein by utilizing Western blot and immunofluorescence analysis. As shown in Fig. 7,  $\alpha$ -ENaC abundance (Fig. 7, A and B) and localization (Fig. 7C) was not different between *osr1*<sup>+/+</sup> and *osr1*<sup>+/KI</sup> mice ( $n = 3$ ).

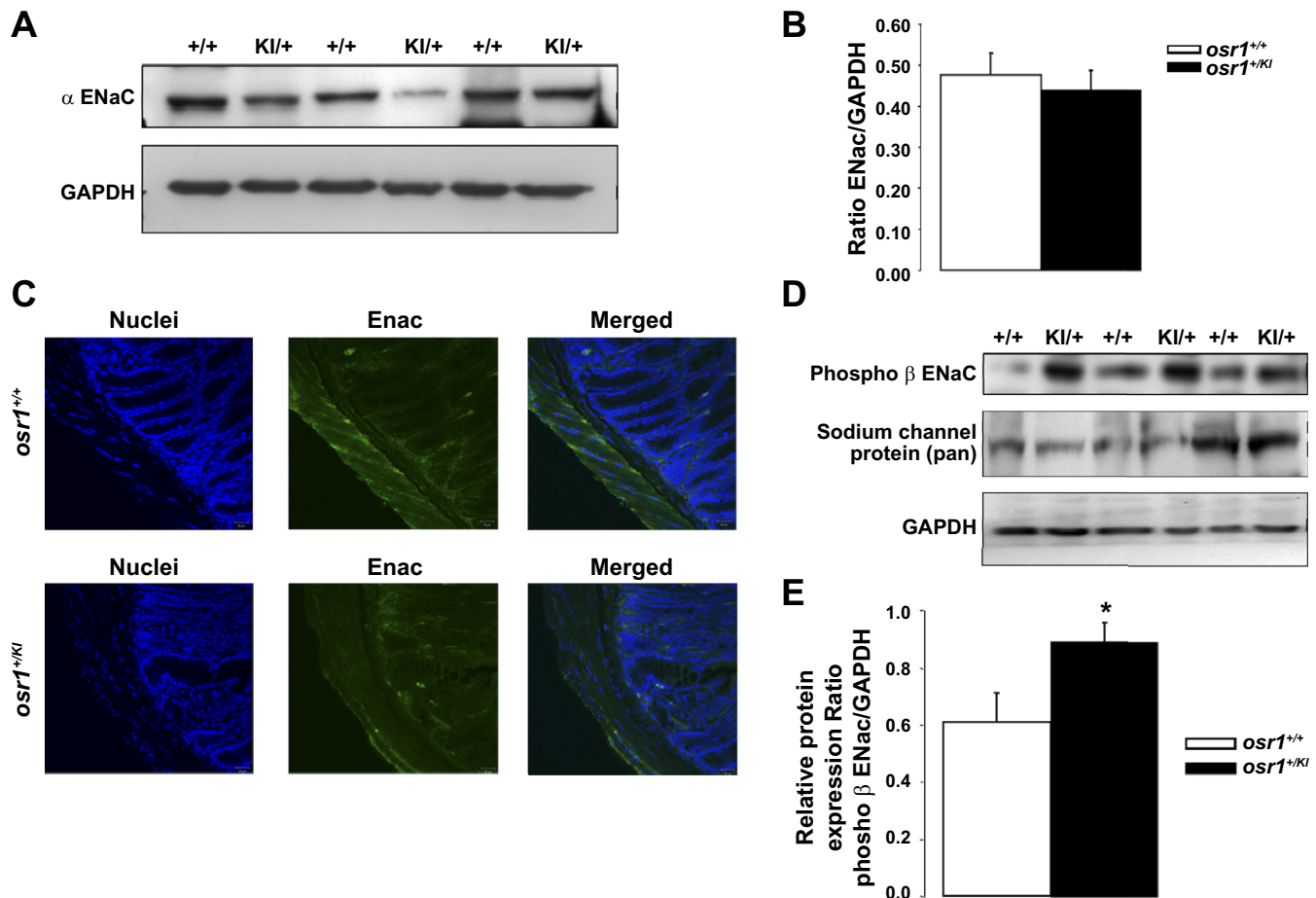


Fig. 7. Expression of epithelium  $\text{Na}^+$  channel (ENaC) in colonic tissue from *osr1*<sup>+/+</sup> and *osr1*<sup>+/KI</sup> mice. A: original Western blot ( $n = 3$  for each genotype) of the expression of  $\alpha$ -ENaC (top) and GAPDH protein (bottom) in the colonic tissue from heterozygous OSR1 knockin mice and wild-type mice. B: arithmetic means  $\pm$  SE ( $n = 3$  for each genotype) of abundance of  $\alpha$ -ENaC (relative to GAPDH) in colonic tissue from *osr1*<sup>+/+</sup> (open bar) and *osr1*<sup>+/KI</sup> (solid bar) mice. C: immunofluorescence of  $\alpha$ -ENaC expression (green) in *osr1*<sup>+/KI</sup> (bottom) and in *osr1*<sup>+/+</sup> mice (top). D: original Western blot ( $n = 7$  for each genotype) of the expression of the phosphorylated  $\beta$ -ENaC (ser633) (top), sodium channel protein pan (middle), and GAPDH protein (bottom) in the colonic tissue from heterozygous OSR1 knockin mice and wild-type mice. E: arithmetic means  $\pm$  SE ( $n = 7$  for each genotype) of abundance of phosphorylated  $\beta$ -ENaC (relative to  $\beta$ -actin) in colonic tissue from *osr1*<sup>+/+</sup> (open bar) and *osr1*<sup>+/KI</sup> (solid bar) mice.



As shown in Fig. 7,  $D$  and  $E$ , phospho- $\beta$ -ENaC (ser 633) was significantly higher in  $osr1^{+/KI}$  ( $n = 7$ ).

## DISCUSSION

The present study reveals that WNK resistance of OSR1 affects small intestinal and colonic  $\text{Na}^+$  reabsorption. Both small intestinal NHE and colonic ENaC activity were significantly higher in OSR1 knockin mice carrying one allele of WNK-insensitive <sup>Thr185Ala</sup> OSR1 mutant ( $osr1^{+/KI}$ ) than in wild-type mice ( $osr1^{+/+}$ ). Accordingly, fecal  $\text{Na}^+$  excretion was significantly lower in  $osr1^{+/KI}$  mice than in  $osr1^{+/+}$  mice.

In theory, the NHE activity in  $osr1^{+/KI}$  small intestine could result from cytosolic acidification, which is known to stimulate NHE activity (19). However, the cytosolic pH was similar in  $osr1^{+/KI}$  mice and in  $osr1^{+/+}$  mice, indicating that the NHE is stimulated by some other mechanism. Alternatively, the stimulation of the NHE in  $osr1^{+/KI}$  could result from cell shrinkage, which stimulates the NHE in parallel to the  $\text{Cl}^-/\text{HCO}_3^-$  exchanger (24, 29). Activation of those two carriers allows the entry of  $\text{NaCl}$ , followed by osmotically obliged water. The  $\text{H}^+$  and  $\text{HCO}_3^-$  extruded in exchange for  $\text{Na}^+$  (NHE) and  $\text{Cl}^-$  ( $\text{Cl}^-/\text{HCO}_3^-$  exchanger) are replenished in the cell by cytosolic formation from  $\text{CO}_2$ , which easily crosses the cell membrane (24, 29). Volume regulatory stimulation of the NHE may result from defective OSR1-dependent stimulation of the  $\text{Na}^+/\text{K}^+/\text{2Cl}^-$  cotransporter in  $osr1^{+/KI}$  cells, because OSR1 is known to stimulate the  $\text{Na}^+/\text{K}^+/\text{2Cl}^-$  cotransporter and to participate in cell volume regulation (3, 7, 9, 16, 26, 27, 40, 53). However, NHE1 rather than NHE3 is implicated in the regulation of cell volume (1).

ENaC-related cation channels are again sensitive to cell volume and activated by cell shrinkage (4, 37). Whether colonic ENaC activity is cell volume sensitive has, however, not been tested thus far.

Besides activation by cell shrinkage, OSR1 may influence NHE activity and ENaC more directly. However, evidence for an inhibitory effect of OSR1 on NHE activity or ENaC has not been published. At least in theory, the enhanced activity of NHE activity and ENaC in  $osr1^{+/KI}$  mice could result from renal salt loss due to compromised activation of thiazide-sensitive  $\text{Na}^+/\text{Cl}^-$  cotransporter and the furosemide-sensitive  $\text{Na}^+/\text{K}^+/\text{2Cl}^-$  cotransporter in the kidney. We did not observe significant differences in water- and electrolyte-regulating hormones between  $osr1^{+/KI}$  mice and  $osr1^{+/+}$  mice. This does not, however, rule out minor changes of hormone release that affect small intestinal transport.

In contrast to NHE and ENaC activity, the glucose-induced current is lower in  $osr1^{+/KI}$  mice than in  $osr1^{+/+}$  mice. In theory, this effect could again reflect an influence of OSR1 on SGLT1 activity or an effect on other carriers and channels indirectly influencing glucose-induced current.

The present observations reveal differences between heterozygous mice and wild-type mice. Homozygous OSR1 knockin mice ( $osr1^{KI/KI}$ ) are not viable (38), highlighting the physiological importance of WNK-sensitive OSR1-dependent regulation. The substantial difference of fecal salt excretion, small intestinal NHE, and colonic ENaC activity between  $osr1^{+/KI}$  mice and  $osr1^{+/+}$  mice underscores the power of WNK-sensitive OSR1-dependent regulation.

In conclusion, small intestinal NHE and colonic ENaC activity are significantly higher in  $osr1^{+/KI}$  than in  $osr1^{+/+}$  mice. The observations thus point to a novel functional role of the OSR1.

## ACKNOWLEDGMENTS

The authors are indebted to Rebecca Lam, Max Planck Institute Frankfurt for critically reading the manuscript. They are further indebted to Dario Alessi from the Medical Research Council Protein Phosphorylation Unit, College of Life Sciences, University of Dundee, Dundee, UK, who kindly provided the mice and the antibodies. The authors further gratefully acknowledge the meticulous preparation of the manuscript by Lejla Subasic, Tanja Loch, and Sari Rube.

## GRANTS

This work was supported by the Deutsche Forschungsgemeinschaft.

## DISCLOSURES

No conflicts of interest, financial or otherwise, are declared by the author(s).

## AUTHOR CONTRIBUTIONS

Author contributions: V.P., G.P., A.F., R.R., D.M., T.P., and I.A. performed experiments; V.P., G.P., A.F., R.R., D.M., A.R., M.F., and F.L. approved final version of manuscript; D.M., A.R., and M.F. analyzed data; A.R., M.F., and F.L. edited and revised manuscript; M.F. interpreted results of experiments; M.F. prepared figures; F.L. conception and design of research; F.L. drafted manuscript.

## REFERENCES

- Alexander RT, Grinstein S.  $\text{Na}^+/\text{H}^+$  exchangers and the regulation of volume. *Acta Physiol (Oxf)* 187: 159–167, 2006.
- Anselmo AN, Earnest S, Chen W, Juang YC, Kim SC, Zhao Y, Cobb MH. WNK1 and OSR1 regulate the  $\text{Na}^+$ ,  $\text{K}^+$ ,  $\text{2Cl}^-$  cotransporter in HeLa cells. *Proc Natl Acad Sci USA* 103: 10883–10888, 2006.
- Anselmo LB, Gross JL, Haddad F, Deheinzeln D, Younes RN, Barbuto JA. Functional analysis of cells obtained from bronchoalveolar lavage fluid (BALF) of lung cancer patients. *Life Sci* 76: 2945–2951, 2005.
- Bondarava M, Li T, Endl E, Wehner F.  $\alpha$ -ENaC is a functional element of the hypertonicity-induced cation channel in HepG2 cells and it mediates proliferation. *Pflügers Arch* 458: 675–687, 2009.
- Boyarsky G, Ganz MB, Sterzel RB, Boron WF. pH regulation in single glomerular mesangial cells. I. Acid extrusion in absence and presence of  $\text{HCO}_3^-$ . *Am J Physiol Cell Physiol* 255: C844–C856, 1988.
- Choe KP, Strange K. Evolutionarily conserved WNK and Ste20 kinases are essential for acute volume recovery and survival after hypertonic shrinkage in *Caenorhabditis elegans*. *Am J Physiol Cell Physiol* 293: C915–C927, 2007.
- Delpire E, Gagnon KB. SPAK and OSR1, key kinases involved in the regulation of chloride transport. *Acta Physiol (Oxf)* 187: 103–113, 2006.
- Delpire E, Gagnon KB. Genome-wide analysis of SPAK/OSR1 binding motifs. *Physiol Genomics* 28: 223–231, 2007.
- Delpire E, Gagnon KB. SPAK and OSR1: STE20 kinases involved in the regulation of ion homeostasis and volume control in mammalian cells. *Biochem J* 409: 321–331, 2008.
- Dimke H. Exploring the intricate regulatory network controlling the thiazide-sensitive  $\text{NaCl}$  cotransporter (NCC). *Pflügers Arch* 462: 767–777, 2011.
- Falin RA, Morrison R, Ham AJ, Strange K. Identification of regulatory phosphorylation sites in a cell volume- and Ste20 kinase-dependent  $\text{Cl}^-$  anion channel. *J Gen Physiol* 133: 29–42, 2009.
- Flatman PW. Cotransporters, WNKs and hypertension: important leads from the study of monogenetic disorders of blood pressure regulation. *Clin Sci (Lond)* 112: 203–216, 2007.
- Flatman PW. Cotransporters, WNKs and hypertension: an update. *Curr Opin Nephrol Hypertens* 17: 186–192, 2008.
- Furgeson SB, Linas S. Mechanisms of type I and type II pseudohypoaldosteronism. *J Am Soc Nephrol* 21: 1842–1845, 2010.
- Gagnon KB, Rios K, Delpire E. Functional insights into the activation mechanism of Ste20-related kinases. *Cell Physiol Biochem* 28: 1219–1230, 2011.

16. Gimenez I. Molecular mechanisms and regulation of furosemide-sensitive Na-K-Cl cotransporters. *Curr Opin Nephrol Hypertens* 15: 517–523, 2006.
17. Glover M, O'Shaughnessy KM. SPAK and WNK kinases: a new target for blood pressure treatment? *Curr Opin Nephrol Hypertens* 20: 16–22, 2011.
18. Glover M, Zuber AM, O'Shaughnessy KM. Hypertension, dietary salt intake, and the role of the thiazide-sensitive sodium chloride transporter NCCT. *Cardiovasc Ther* 29: 68–76, 2011.
19. Grinstein S, Cohen S, Goetz JD, Rothstein A. Na<sup>+</sup>/H<sup>+</sup> exchange in volume regulation and cytoplasmic pH homeostasis in lymphocytes. *Fed Proc* 44: 2508–2512, 1985.
20. Haas BR, Cuddapah VA, Watkins S, Rohn KJ, Dy TE, Sontheimer H. With-No-Lysine Kinase 3 (WNK3) stimulates glioma invasion by regulating cell volume. *Am J Physiol Cell Physiol* 301: C1150–C1160, 2011.
21. He P, Yun CC. Mechanisms of the regulation of the intestinal Na<sup>+</sup>/H<sup>+</sup> exchanger NHE3. *J Biomed Biotechnol* 2010: 238080, 2010.
22. Hengl T, Kaneko H, Dauner K, Vocke K, Frings S, Mohrlen F. Molecular components of signal amplification in olfactory sensory cilia. *Proc Natl Acad Sci USA* 107: 6052–6057, 2010.
23. Hoffmann EK. Ion channels involved in cell volume regulation: effects on migration, proliferation, and programmed cell death in non adherent EAT cells and adherent ELA cells. *Cell Physiol Biochem* 28: 1061–1078, 2011.
24. Hoffmann EK, Lambert IH, Pedersen SF. Physiology of cell volume regulation in vertebrates. *Physiol Rev* 89: 193–277, 2009.
25. Hoffmann EK, Schettino T, Marshall WS. The role of volume-sensitive ion transport systems in regulation of epithelial transport. *Comp Biochem Physiol A Mol Integr Physiol* 148: 29–43, 2007.
26. Huang CL, Yang SS, Lin SH. Mechanism of regulation of renal ion transport by WNK kinases. *Curr Opin Nephrol Hypertens* 17: 519–525, 2008.
27. Kahle KT, Rinehart J, Lifton RP. Phosphoregulation of the Na-K-2Cl and K-Cl cotransporters by the WNK kinases. *Biochim Biophys Acta* 1802: 1150–1158, 2010.
28. Kunzelmann K, Mall M. Electrolyte transport in the mammalian colon: mechanisms and implications for disease. *Physiol Rev* 82: 245–289, 2002.
29. Lang F, Busch GL, Ritter M, Volkl H, Waldegger S, Gulbins E, Haussinger D. Functional significance of cell volume regulatory mechanisms. *Physiol Rev* 78: 247–306, 1998.
30. McCormick JA, Mutig K, Nelson JH, Saritas T, Hoorn EJ, Yang CL, Rogers S, Curry J, Delpire E, Bachmann S, Ellison DH. A SPAK isoform switch modulates renal salt transport and blood pressure. *Cell Metab* 14: 352–364, 2011.
31. Mercier-Zuber A, O'Shaughnessy KM. Role of SPAK and OSR1 signalling in the regulation of NaCl cotransporters. *Curr Opin Nephrol Hypertens* 20: 534–540, 2011.
32. Moriguchi T, Urushiyama S, Hisamoto N, Iemura S, Uchida S, Natsumo T, Matsumoto K, Shibuya H. WNK1 regulates phosphorylation of cation-chloride-coupled cotransporters via the STE20-related kinases, SPAK and OSR1. *J Biol Chem* 280: 42685–42693, 2005.
33. Pacheco-Alvarez D, Gamba G. WNK3 is a putative chloride-sensing kinase. *Cell Physiol Biochem* 28: 1123–1134, 2011.
34. Park HW, Nam JH, Kim JY, Namkung W, Yoon JS, Lee JS, Kim KS, Venglovecz V, Gray MA, Kim KH, Lee MG. Dynamic regulation of CFTR bicarbonate permeability by [Cl<sup>-</sup>]<sub>i</sub> and its role in pancreatic bicarbonate secretion. *Gastroenterology* 139: 620–631, 2010.
35. Pedersen NB, Hofmeister MV, Rosenbaek LL, Nielsen J, Fenton RA. Vasopressin induces phosphorylation of the thiazide-sensitive sodium chloride cotransporter in the distal convoluted tubule. *Kidney Int* 78: 160–169, 2010.
36. Piechotta K, Garbarini N, England R, Delpire E. Characterization of the interaction of the stress kinase SPAK with the Na<sup>+</sup>-K<sup>+</sup>-2Cl<sup>-</sup> cotransporter in the nervous system: evidence for a scaffolding role of the kinase. *J Biol Chem* 278: 52848–52856, 2003.
37. Plettenberg S, Weiss EC, Lemor R, Wehner F. Subunits  $\alpha$ ,  $\beta$  and  $\gamma$  of the epithelial Na<sup>+</sup> channel (ENaC) are functionally related to the hypertonicity-induced cation channel (HICC) in rat hepatocytes. *Pflügers Arch* 455: 1089–1095, 2008.
38. Rafiqi FH, Zuber AM, Glover M, Richardson C, Fleming S, Jovanovic S, Jovanovic A, O'Shaughnessy KM, Alessi DR. Role of the WNK-activated SPAK kinase in regulating blood pressure. *EMBO Mol Med* 2: 63–75, 2010.
39. Rexhepaj R, Artunc F, Grahammer F, Nasir O, Sandu C, Friedrich B, Kuhl D, Lang F. SGK1 is not required for regulation of colonic ENaC activity. *Pflügers Arch* 453: 97–105, 2006.
40. Richardson C, Alessi DR. The regulation of salt transport and blood pressure by the WNK-SPAK/OSR1 signalling pathway. *J Cell Sci* 121: 3293–3304, 2008.
41. Roos A, Boron WF. Intracellular pH. *Physiol Rev* 61: 296–434, 1981.
42. Rotte A, Pasham V, Eichenmüller M, Yang W, Qadri SM, Bhandaru M, Lang F. Regulation of basal gastric acid secretion by the glycogen synthase kinase GSK3. *J Gastroenterol* 45: 1022–1032, 2010.
43. Salter RD, Watkins SC. Dendritic cell altered states: what role for calcium? *Immunol Rev* 231: 278–288, 2009.
44. Sandu C, Artunc F, Palmada M, Rexhepaj R, Grahammer F, Hussain A, Yun C, Alessi DR, Lang F. Impaired intestinal NHE3 activity in the PDK1 hypomorphic mouse. *Am J Physiol Gastrointest Liver Physiol* 291: G868–G876, 2006.
45. Schwark JR, Jansen HW, Lang HJ, Krick W, Burckhardt G, Hropot M. S3226, a novel inhibitor of Na<sup>+</sup>/H<sup>+</sup> exchanger subtype 3 in various cell types. *Pflügers Arch* 436: 797–800, 1998.
46. Sohara E, Rai T, Yang SS, Ohta A, Naito S, Chiga M, Nomura N, Lin SH, Vandewalle A, Ohta E, Sasaki S, Uchida S. Acute insulin stimulation induces phosphorylation of the Na-Cl cotransporter in cultured distal mpkDCT cells and mouse kidney. *PLoS One* 6: e24277, 2011.
47. Solomon A, Bandhakavi S, Jabbar S, Shah R, Beitel GJ, Morimoto RI. *Caenorhabditis elegans* OSR-1 regulates behavioral and physiological responses to hyperosmotic environments. *Genetics* 167: 161–170, 2004.
48. Thastrup JO, Rafiqi FH, Pozo-Guisado E, Deak M, Vitari AC, Mehellou Y, Alessi DR. SPAK/OSR1 regulate NKCC1 and WNK activity: analysis of WNK isoform interactions and activation by T-loop trans-autophosphorylation. *Biochem J* 441: 325–337, 2012.
49. Uchida S. Pathophysiological roles of WNK kinases in the kidney. *Pflügers Arch* 460: 695–702, 2010.
50. Villa F, Deak M, Alessi DR, van Aalten DM. Structure of the OSR1 kinase, a hypertension drug target. *Proteins* 73: 1082–1087, 2008.
51. Villa F, Goebel J, Rafiqi FH, Deak M, Thastrup J, Alessi DR, van Aalten DM. Structural insights into the recognition of substrates and activators by the OSR1 kinase. *EMBO Rep* 8: 839–845, 2007.
52. Vitari AC, Deak M, Morrice NA, Alessi DR. The WNK1 and WNK4 protein kinases that are mutated in Gordon's hypertension syndrome phosphorylate and activate SPAK and OSR1 protein kinases. *Biochem J* 391: 17–24, 2005.
53. Vitari AC, Thastrup J, Rafiqi FH, Deak M, Morrice NA, Karlsson HK, Alessi DR. Functional interactions of the SPAK/OSR1 kinases with their upstream activator WNK1 and downstream substrate NKCC1. *Biochem J* 397: 223–231, 2006.
54. Waisbren SJ, Geibel J, Boron WF, Modlin IM. Luminal perfusion of isolated gastric glands. *Am J Physiol Cell Physiol* 266: C1013–C1027, 1994.
55. Wheeler JM, Thomas JH. Identification of a novel gene family involved in osmotic stress response in *Caenorhabditis elegans*. *Genetics* 174: 1327–1336, 2006.
56. Wilson FH, Disse-Nicodeme S, Choate KA, Ishikawa K, Nelson-Williams C, Desitter I, Gunel M, Milford DV, Lipkin GW, Achard JM, Feely MP, Dussol B, Berland Y, Unwin RJ, Mayan H, Simon DB, Farfel Z, Jeunemaitre X, Lifton RP. Human hypertension caused by mutations in WNK kinases. *Science* 293: 1107–1112, 2001.
57. Yang SS, Morimoto T, Rai T, Chiga M, Sohara E, Ohno M, Uchida K, Lin SH, Moriguchi T, Shibuya H, Kondo Y, Sasaki S, Uchida S. Molecular pathogenesis of pseudohypoaldosteronism type II: generation and analysis of a Wnk4(D561A/+) knockin mouse model. *Cell Metab* 5: 331–344, 2007.
58. Zachos NC, Tse M, Donowitz M. Molecular physiology of intestinal Na<sup>+</sup>/H<sup>+</sup> exchange. *Annu Rev Physiol* 67: 411–443, 2005.
59. Zagorska A, Pozo-Guisado E, Boudeau J, Vitari AC, Rafiqi FH, Thastrup J, Deak M, Campbell DG, Morrice NA, Prescott AR, Alessi DR. Regulation of activity and localization of the WNK1 protein kinase by hyperosmotic stress. *J Cell Biol* 176: 89–100, 2007.